

Reuse, Don't Retrain: A Recipe for Continued Pretraining of Language Models

Anonymous ACL submission

Abstract

As language models have scaled both their number of parameters and pretraining dataset sizes, the computational cost for pretraining has become intractable except for the most well-resourced teams. This increasing cost makes it ever more important to be able to reuse a model after it has completed pretraining; allowing for a model's abilities to further improve without needing to train from scratch. In this work, we detail a set of guidelines that cover how to design efficacious data distributions and learning rate schedules for continued pretraining of language models. When applying these findings within a continued pretraining run on top of a well-trained 15B parameter model, we show an improvement of 9% in average model accuracy compared to the baseline of continued training on the pretraining set. The resulting recipe provides a practical starting point with which to begin developing language models through reuse rather than retraining.

1 Introduction

Language modeling abilities have seen massive improvements over the past few years (Brown et al., 2020; Chowdhery et al., 2022; OpenAI, 2024; Team, 2024). While these advancements have enabled language models (LMs) to become highly-skilled conversational agents (OpenAI, 2024; Anthropic, 2024; Team, 2024), they have come with increased computational cost as pretraining has become ever more expensive due to both the number of model parameters (Team et al., 2024; DeepSeek-AI et al., 2024) and pretraining dataset size (Touvron et al., 2023; Gemma Team, 2024; Parmar et al., 2024) continuing to grow in scale. With new LMs that set state of the art accuracy being released on a frequent basis, LMs developed only a couple months back are becoming obsolete as their capabilities are no longer up to par. This leaves model developers with the choice of either pretraining new LMs from scratch or reusing their existing

LMs and updating them with new information in order to match current best LM abilities.

Due to the large computational cost that pretraining of modern LMs incurs, frequent complete retraining is intractable. This makes the reuse of already developed LMs via continued pretraining an attractive proposition. While most recent works (Ibrahim et al., 2024; Jang et al., 2022; Ke et al., 2023; Çağatay Yıldız et al., 2024) have recommended guidelines for continued pretraining when adapting language models to new data domains or distribution shifts, intuition or recommendations on how to improve a model's general purpose abilities from a previously finalized checkpoint with continued pretraining have not been widely explored. In this paper, we focus on this under-studied setting and identify strategies that allow for already trained LMs to improve upon areas of weakness without experiencing degradations in other capabilities.

In our experiments, we start on top of a 15B parameter LM that has seen 8T tokens of pretraining data. Experimenting with a well trained model of this scale ensures that our findings will be transferable to most settings and model sizes. We first identify the type of data distribution that should be used during continued pretraining and find that it is optimal to have two distributions, with the final one more heavily weighting data sources that relate to the abilities we want to improve in the model. Second, we determine what learning rate schedules enable the most efficient learning during continued pretraining and determine that the most performant one strikes a balance between magnitude of learning rate and steepness of decay. Lastly, we show how the learning rate value at which we switch between data distributions affects downstream accuracy and identify the point at which this switch should be made.

These findings culminate in a recipe that can be used to perform continued pretraining to improve the capabilities of an existing LM. We demonstrate

that this recipe is beneficial at continued training scales from 100B to 1 trillion tokens, illustrating its flexibility and robustness to be used in a wide variety of settings. We hope that this recipe will allow for model providers to forgo the need to regularly retrain models from scratch as it makes it possible to reuse a trained model to attain improved capabilities.

2 Related Works

Continued training methods aim to take an already trained model and incorporate new data, adapt it for a given domain, or specialize it on a certain task (Rolnick et al., 2019; Caccia et al., 2021; Lesort et al., 2022; Gupta et al., 2023; Lin et al., 2024). The major challenge that arises during continued training is enabling a model to learn new information without forgetting previously attained knowledge or capabilities (Robins, 1995; French, 1999). The learning rate schedule and data distribution used during continued training (Gupta et al., 2023; Ibrahim et al., 2024; Winata et al., 2023; Scialom et al., 2022) have been shown to be particularly important in preventing such catastrophic forgetting.

For LMs, one major setting of continued training has been to embed more recent knowledge into the model by using data collected at a date later than when the pretraining set was constructed (Jin et al., 2022; Jang et al., 2022, 2023; Loureiro et al., 2022; Qin et al., 2022). Results from these studies found that using experience replay (Chaudhry et al., 2019) and knowledge distillation (Hinton et al., 2015) are particularly effective. Continued training is also commonly used in LMs to adapt the model to data coming from a new domain (Ke et al., 2023; Gururangan et al., 2020; Wu et al., 2024). Many of these methods for domain adaptive continued training update a portion of the model’s weights with the new data to ensure that previous knowledge is not lost. For instance, (Wu et al., 2024) does so via an expansion of the transformer blocks and only updating the newly added weights.

More related to the setting which we explore, several studies utilize continued pretraining to specialize a LM on a given task or domain (Zan et al., 2022; Yadav et al., 2023; Ma et al., 2023; Yang et al., 2024; Labrak et al., 2024). Despite investigating effective strategies for continued pretraining, these studies differ from ours as they do not aim to improve the general capabilities of LMs, train for far fewer tokens, and use much smaller model

sizes. The main study which offers a comparative setting to ours is (Ibrahim et al., 2024) which provides a recipe, based on learning rate schedule and example replay recommendations, for maintaining general purpose abilities during continued pretraining on data distribution shifts. Their experimental setting consists of a 10B parameter model that was pretrained for 300B tokens. Our study differs from (Ibrahim et al., 2024) as we aim to improve the general capabilities of the LM further, and in our experimental setting we perform continued pretraining for up to 1T tokens with a 15B parameter model that was pretrained on 8T tokens.

3 Experimental Setup

The continued pretraining process is as follows: a model is first pretrained, then a data distribution and learning rate schedule are chosen, a continued pretraining run takes place, and finally the, hopefully improved, model is returned. Before delving into the experiments that define the continued training recipe, we detail the datasets and model architecture that are used.

3.1 Data Sources

3.1.1 Pretraining

Our pretraining dataset consists of three different domains of data: English natural language data, multilingual natural language data, and source code data. Table 1 highlights the data sources that compose the pretraining set along with their respective token counts. In our English corpus, the Web Crawl data is sourced from Common Crawl (CC) snapshots while the remaining categories are comprised of high-quality sets. For instance, the miscellaneous category consists of BigScience ROOTS (Lachaux et al., 2020), Reddit, and Pile-Stories (Gao et al., 2020), the encyclopedia category contains Wikipedia and Stack Exchange, and scientific papers includes ArXiv and PubMed.

The multilingual dataset consists of 53 languages with the majority of examples being drawn from CC snapshots, although a small portion comes from machine translation parallel corpora (Schwenk et al., 2019; El-Kishky et al., 2019). Lastly, our source code data is drawn from permissively licensed GitHub repositories and totals over 43 languages.

We pretrain the model for 8T tokens. Given that current state of the art LMs are pretrained for trillions of tokens, we want to experiment on top of

Data type	Data source	Tokens (B)
English	Web Crawl	5,106
	Misc.	179
	News	93
	Scientific Papers	82
	Books	80
	Legal	50
	Encyclopedia	31
	Finance	20
Multilingual	Web crawl	2,229
	Parallel corpora	55
Source Code	GitHub	583

Table 1: The pretraining data composition. Appendix A.1 and A.2 breakdown the multilingual and coding languages.

a pretrained model that is emblematic of the type of models which the continued pretraining recipe would be used for.

3.1.2 Continued Pretraining

As the most likely scenario in continued pretraining is that the available datasets are exactly those which made up the pretraining set, the vast majority of our continued training data blend is comprised of the pretraining data sources. The only new additional source of data is a set of question and answer (QA), alignment style examples. Such examples have been shown to better extract stored knowledge within LMs (Allen-Zhu and Li, 2023). This set of QA data totals 2.8B tokens and Table 2 highlights the categories of types of QA examples.

Data type	Data source	Tokens (B)
QA	World Knowledge	1.13
	Reasoning	0.92
	STEM	0.31
	Chat	0.26
	Code	0.19

Table 2: The five constituent categories of the QA, alignment style data.

3.2 Model Architecture and Hyperparameters

We experiment using a 15B parameter decoder-only transformer (Vaswani et al., 2017) LM with causal attention masks. It has 3.2 billion embedding parameters and 12.5 billion non-embedding parameters. Additional architectural specifications

include: 32 transformer layers, a hidden size of 6144, 48 attention heads, Rotary Position Embeddings (RoPE) (Su et al., 2023), squared ReLU activations in the MLP layers, a SentencePiece (Kudo and Richardson, 2018) tokenizer with a vocabulary size of 256k, no bias terms, and untied input-output embeddings. Additionally, we use grouped query attention (GQA) (Ainslie et al., 2023) with 8 KV heads.

The model is pretrained with a sequence length of 4,096 and uses batch size rampup over the first 5% of pretraining tokens, starting from a batch size of 384 and building up to one of 1,152. We use a cosine learning rate schedule, with warmup of 16B tokens, to decay from a maximum learning rate (LR) of $\eta_{max} = 4.5e-4$ to $\eta_{min} = 4.5e-5$. We train using the AdamW (Loshchilov and Hutter, 2019) optimizer with $\beta_1 = 0.9$, $\beta_2 = 0.95$, and a weight decay of 0.1. In continued pretraining, the only hyperparameter that is altered is the learning rate schedule.

3.3 Evaluation

We evaluate the model using a representative set of tasks to test its change in abilities across the English, multilingual, and coding domains. To assess English capabilities, we evaluate on the widely-used MMLU (Hendrycks et al., 2020) and Hellaswag (Zellers et al., 2019) benchmarks. MMLU measures the model’s world knowledge across 57 domains while Hellaswag assesses commonsense reasoning ability within natural language inference. For our multilingual evaluations, we use the Multilingual Grade School Mathematics (MGSM) (Shi et al., 2022) benchmark and specifically report the average accuracy across the language subset of Spanish, Japanese, and Thai, as they represent a high, medium, and low resource language respectively. Lastly, to assess the model’s coding capabilities we utilize the Python code generation task of HumanEval (Chen et al., 2021) with evaluations reported in the pass@1 (Kulal et al., 2019) setting. In our results below, we report the average score across all four of these tasks with fully detailed evaluation scores shared in the Appendix.

4 Continued Pretraining Recipe

The experimental findings which constitute our continued pretraining recipe are shared below:

Recipe

- Start with a data distribution that is similar to the pretraining set but places larger weight on high quality sources before transitioning to a second distribution that incorporates QA data and upweights sources in areas of model weakness.
- The learning rate schedule should start from η_{min} of the pretrained model and decay with cosine annealing to $\frac{\eta_{min}}{100}$.
- The switch between data distribution should occur at $\frac{\eta_{max}}{5}$ in the learning rate schedule.

5 Experiments

The results of the pretrained base model are shown in Table 3. The aim for our continuous training recipe will be to define steps that help maximally improve upon this benchmark. All detailed experiments perform continuous pretraining for 300B tokens. Additionally, we note that in our experiments we choose to load in the optimizer state from the pretrained model as we found that there was a negligible difference in evaluation accuracy when the optimizer state was loaded in or when initialized from scratch. Thus, we expect that whether eventual practitioners have the optimizer state of the pretrained model available or not, the resulting findings will hold.

Model	Average Accuracy
Pretrained	48.9

Table 3: Model accuracy after 8T tokens of pretraining. In per-task evaluations scores shared in Table 12, we find the model particularly struggles on tasks that assess STEM based reasoning capabilities.

5.1 Data Distribution

A crucial component of any training run is the data distribution – it defines the information which a model sees and directly impacts the model’s capabilities. As continuous pretraining builds on top of a model which has already seen a given pretraining distribution, it is important to define a data distribution which allows the model to learn new concepts without also deviating too far from the pretraining distribution such that the model begins to

experience training instability and accuracy regression. Through a series of runs which tackle what compositions of data distributions best improve the abilities of a pretrained model, we identify general characteristics that can be applied across most continuous pretraining scenarios. In these experiments, we use a learning rate schedule that starts from η_{min} and decays to 0 with cosine annealing.

First, we examine if the inclusion of QA data, which improves the ability of a model to extract stored knowledge (Allen-Zhu and Li, 2023), improves model accuracy. Coupled with this question is another on how to best incorporate the QA data, or more generally any dataset which is not contained within the pretraining data distribution, into the continued training run: immediately at the beginning and throughout the entirety of continued training, or rather reserved till the end of continued training following a curriculum learning setup (Soviany et al., 2022; Blakeney et al., 2024). We hypothesize that inclusion of new data sources at the beginning of continued pretraining allows for the model to best learn the new information, but may cause learning instabilities that could be mitigated by showing the new dataset at the end of the run when the learning rate is less aggressive. To answer these questions, we compare continued training entirely with the pretraining data blend, entirely with a QA data blend, and with a mix of the pretraining and QA data blends where we start with the pretraining blend and switch to the QA data blend late in the training run. The QA data blend in this scenario adds the QA dataset to the pretraining data distribution with a weight of 10%.

Data Blend	Avg. Acc.
Pretraining	51.5
QA	53.4
Pretraining (250B), QA (50B)	54.3

Table 4: Using two data distributions, with the QA data appearing in the latter, leads to the largest improvement via continued pretraining. () indicates the number of training tokens for each blend. Per-task evaluations scores are shared in Table 13.

Table 4 illustrates that the incorporation of QA data markedly outperforms solely using existing data from the pretraining set. Additionally, first using the pretraining data blend for the majority of training tokens before transitioning to the QA data blend at the end of continued pretraining ex-

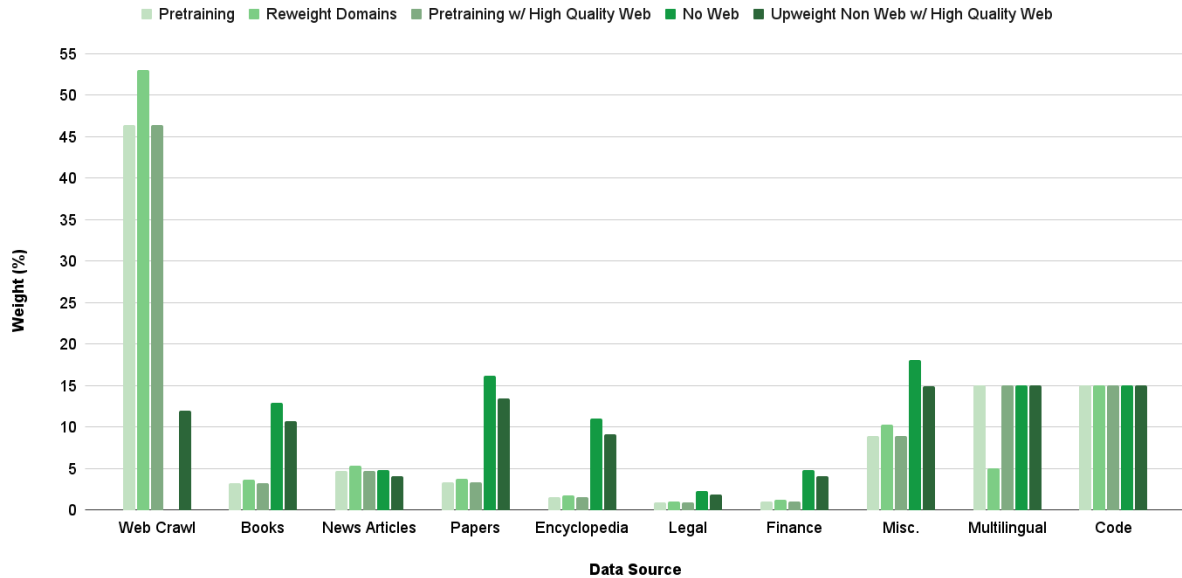


Figure 1: Breakdown of the various distributions considered for the General Blend (GB). We use Upweight Non Web w/ High Quality Web as the GB moving forward given its strong performance across all evaluation areas.

316 hibits improved accuracy compared to using the
 317 QA blend throughout the entirety of training. This
 318 indicates that continued pretraining runs should
 319 begin with a data distribution which more closely
 320 aligns to the pretraining one followed by a blend
 321 that then introduces new data. Moving forward,
 322 we refer to the initial blend as the general blend,
 323 GB, and the latter blend as the QA blend, QB, and
 324 discuss how they can be refined to realize further
 325 improvements.

326 We hypothesize that the optimal GB will be one
 327 which places greater emphasis on high quality data
 328 sources and areas of model weakness, without devi-
 329 ating too far from the pretraining distribution.
 330 Such a blend will enhance knowledge in needed ar-
 331 eas and prime the model for the QB blend without
 332 worry of experiencing large training instabilities.
 333 Figure 1 illustrates the various GB distributions we
 334 consider; in addition to upweighting sources of in-
 335 terest, we either subset web crawl to just high qual-
 336 ity documents, as identified by being in the bottom
 337 quartile of perplexity scores from a KenLM model
 338 (Heafield, 2011) trained on Wikipedia, or remove
 339 web crawl altogether. Experimenting with the vari-
 340 ous GB distributions for all 300B tokens of contin-
 341 ued training, Table 5 shows that each improves
 342 upon the pretraining distribution. Even though it
 343 does not achieve the highest average accuracy, we
 344 choose Upweight Non Web with High Quality Web
 345 as the GB moving forward, because compared to
 346 others, it most consistently achieves high scores

across all considered tasks as shown in Table 13.

Data Blend	Avg. Acc.
Pretraining	51.5
Reweight Domains	51.7
Pretraining w/ High Quality Web	52.5
No Web	52.9
UW Non Web w/ High Quality Web	52.0

Table 5: Evaluation results of various GB candidate distributions. Per-task evaluations scores are shared in Table 13

348 With a GB distribution in place, we now look
 349 to define the QB distribution by first refining the
 350 weights placed on the sources within the QA data
 351 and then optimizing the QB distribution as a whole.
 352 In the initial QB distribution, the QA data was
 353 added as is, and this weighting is shown as QA
 354 blend 1 in Figure 2. Given that the pretrained model
 355 struggles on STEM tasks, we create two additional
 356 blends that both upweight the QA STEM data while
 357 either maintaining the original weight of QA world
 358 knowledge, blend 2, or QA chat, blend 3, data as
 359 seen in Figure 2. We choose to maintain the weight
 360 in world knowledge and chat information as such
 361 examples cover a broad range of topics and help
 362 better align model responses to questions respec-
 363 tively. Table 6 highlights that upon adding each of
 364 the QA blends to the initial QB distribution follow-
 365 ing 250B tokens of the identified GB, QA data that
 366 emphasizes both STEM and chat information leads

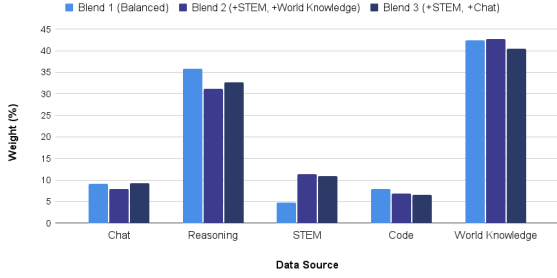


Figure 2: Various distributions of QA data. We use Blend 3.

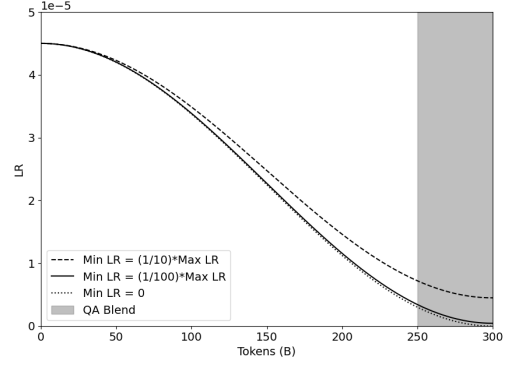


Figure 3: Cosine decay schedules with a Max LR of $4.5e-5$. Each schedule differently prioritizes LR magnitude and slope of decay.

to the best results.

Data Blend	Avg. Acc.
QA 1	54.3
QA 2 (+STEM, +World Knowledge)	53.0
QA 3 (+STEM, +Chat)	54.9

Table 6: Evaluation results of various QA blend candidates. Per-task evaluations scores are shared in Table 13

We now incorporate the QA data within the overall QB distribution. In previous runs, the QB distribution, aside from the QA dataset, exactly mirrored the pretraining set. We define a new series of distributions based on more aggressive upweighting of sources in areas of model weakness and amount of weight placed on the QA dataset as seen in Figure 4. Table 7 details that the aggressive weighting in the QB is beneficial, and we use the QB termed QA blend moving forward. With refined GB and QB distributions, the average evaluation accuracy has improved from 48.9 for the pretrained model to 55.4, a 13% improvement.

Data Blend	Avg. Acc.
Pretraining blend w/ QA data	54.3
General blend w/ QA data	54.2
QA	55.4
QA w/ Upweighted STEM	54.4
QA w/ 1.5e QA data	54.9
QA w/ 3.5e QA data	54.4

Table 7: Evaluation results of various QB candidate distributions. Per-task evaluations scores are shared in Table 13

5.2 Learning Rate Schedule

The learning rate schedule greatly impacts the training dynamics and efficacy of continued pretraining

(Gupta et al., 2023; Ibrahim et al., 2024; Winata et al., 2023).

In our above continued pretraining experiments, the learning rate schedule starts at a maximum LR of $\eta_{max_{ct}} = 4.5e-5$, which is equal to η_{min} , and decays to a minimum LR of 0 using cosine annealing. As seen in Figure 3, a minimum LR of 0 facilitates a steep slope of decay but the magnitude of LR is severely impacted, especially over the tokens where the QB is used which may impact the model’s ability to extract full utility from the QA data. To understand the trade-off between these two characteristics of the learning rate schedule in continued pretraining runs, we experiment with two additional minimum learning rate values: $\frac{\eta_{max_{ct}}}{10} = 4.5e-6$ and $\frac{\eta_{max_{ct}}}{100} = 4.5e-7$.

LR Schedule	Avg. Acc.
Decay to $\frac{\eta_{max_{ct}}}{10}$	54.8
Decay to $\frac{\eta_{max_{ct}}}{100}$	55.7
Decay to 0	55.4

Table 8: Evaluation results of learning rate schedules with varying Min LR values. Per-task evaluations scores are shared in Table 14

Table 8 highlights that it is in fact best to strike a middle ground between magnitude of LR and slope of decay, as a minimum LR of $\frac{\eta_{max_{ct}}}{100}$ achieves the best accuracy. Such a minimum LR value allows for a learning rate schedule that has reasonable decay over the QB tokens, unlike when using a minimum LR of $\frac{\eta_{max_{ct}}}{10}$, without severely sacrificing on magnitude of LR, as was the case with a minimum LR of 0.

Experiments with varying learning rate warmup

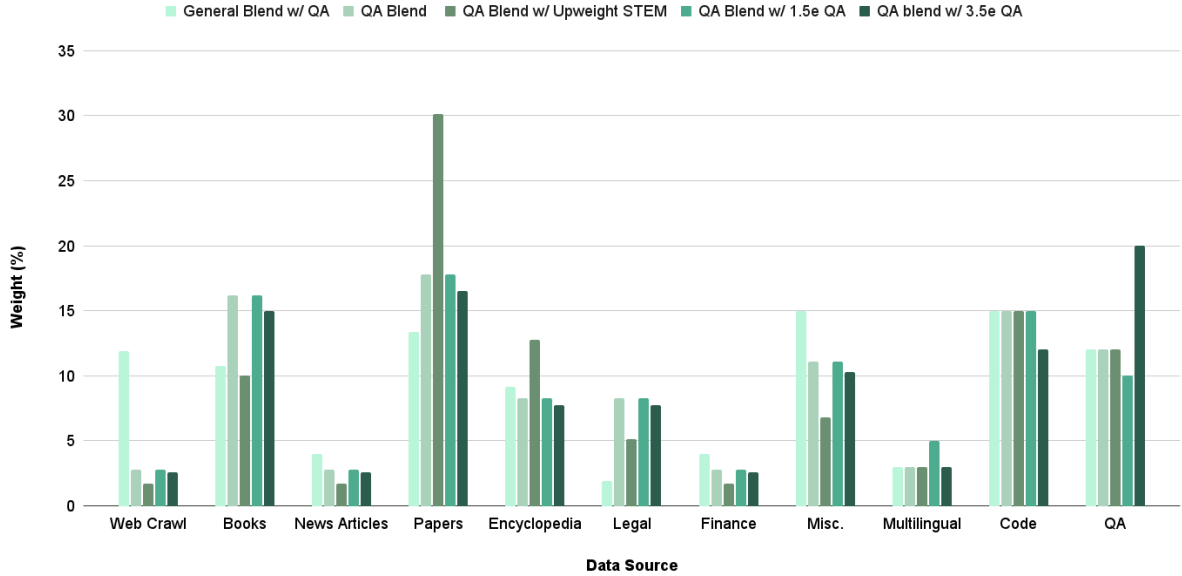


Figure 4: Breakdown of the various distributions considered for the QB. N_e refers to N epochs of the QA data. The final chosen distribution is shown as QA Blend which used 2 epochs of QA data.

and maximum LR values led to accuracy regressions compared to the schedule detailed above. In addition, we ran ablations with a different annealing schedule, WSD (Hu et al., 2024), however the results were not competitive to cosine annealing. Full details and results for both studies are shared in Appendix B.2.

5.3 Switch of Data Distributions

Until this point, we have been switching between the GB and the QB after 250B tokens of continued pretraining. We believe this to be sub-optimal, as it is unclear how switching between distributions after a fixed number of tokens can be easily translated to continued training runs of different token horizons. We hypothesize that the optimal point for switching between the data distributions depends upon the learning rate schedule. Figure 5 highlights how both the number of tokens and learning rate values for the QB blend would differ if the distribution switch occurred at progressively smaller fractions of the maximum LR. As the fraction goes to 0, both the slope of decay and magnitude of the learning rate shrink, meaning that there likely is an optimal point in the learning rate curve where both of these characteristics are still conducive to enable learning but also not too aggressive to the point where the data shift in the QB distribution causes training instability.

Table 9 highlights that switching between the GB and QB at $\frac{\eta_{max_{ct}}}{5}$ achieves the best accuracy and improves upon the heuristically chosen switch

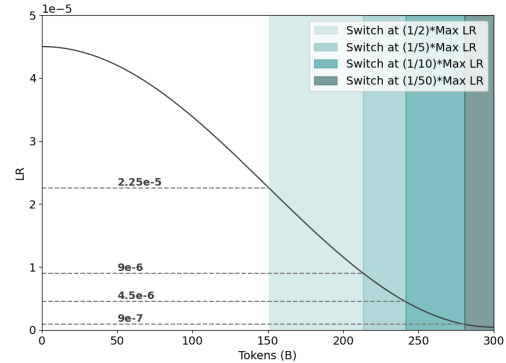


Figure 5: Relationship between different distribution switch points and the number of QB tokens.

point by 0.4 points on average. Wanting to confirm this distribution switch point holds at differing amounts of continued pretraining tokens, we ran an ablation on a scale of 100B tokens and found that $\frac{\eta_{max_{ct}}}{5}$ again maximized the results as seen in Table 18.

Distribution Switch	Avg. Acc.
At $\eta_{max_{ct}}$ (from step 0)	52.8
At $\frac{\eta_{max_{ct}}}{2}$	54.7
At $\frac{\eta_{max_{ct}}}{5}$	56.1
At $\frac{\eta_{max_{ct}}}{10}$	55.0
At $\frac{\eta_{max_{ct}}}{50}$	54.6

Table 9: Evaluation results of varying distribution switch points. Per-task evaluations scores are shared in Table 17

This finalizes our continued pretraining recipe. We highlight the utility of this recipe as it allows the model to achieve an average accuracy of 56.1, which improves upon the natural baseline of continued training on the pretraining distribution, as shared in Table 4, by 9%.

6 Ablations

6.1 Varying Token Horizons

We show the efficacy of the identified continued pretraining recipe when used at varying numbers of continued training tokens. Table 10 illustrates that on continued training horizons from 100B to 1T tokens, the identified recipe consistently achieves improved evaluation results – realizing a 16% gain over the pretrained model when using 1T tokens of continued training. We do note that the slope in accuracy improvement from 300B to 1T tokens is lower than that from 100B to 300B tokens, we hypothesize that as we are mainly reusing documents from the pretraining set when doing a large number of continued training tokens the repeated number of epochs on the same data sources have decreasing marginal utility.

Num CPT Tokens	MMLU	Avg. Acc.
0B	59.3	48.9
100B	63.0	55.0
300B	63.8	56.1
1T	65.3	56.8

Table 10: Performance of the continuous pretraining (CPT) recipe across different token horizons. Per-task evaluations scores are shared in Table 19

6.2 Document Mining

In an effort to improve the utility of the data sources that are seen for multiple epochs in long horizon continued pretraining runs, we aim to find a subset of examples that are most helpful for model improvement. As the QA dataset was shown to significantly boost model accuracies, we hypothesize that restricting each pretraining data source to the set of documents which are most similar to the QA examples would be beneficial. To do so, we use the E5-large-v2 (Wang et al., 2022) text embedding model to obtain an embedding for each document in our pretraining and QA sets. Using the Faiss library (Johnson et al., 2017), we efficiently perform a 50-nearest neighbor search across all these

embeddings to obtain the 50 most similar, non-QA documents to each example in the QA set. The identified subset of examples constitutes 60B tokens, and we term this approach document mining.

Table 11 shows a training run where we replace all non-QA data sources in the QB distribution solely with the examples identified via document mining. We find that these documents substantially improve the performance of the continued pretraining run and believe that document mining is a viable approach at extracting further utility from existing data sources.

Blend	MMLU	Avg. Acc.
CT 1T	65.3	56.8
CT 1T w/ Mined Docs	66.6	57.9

Table 11: Mining examples related to QA documents further improves accuracy. Per-task evaluations scores are shared in Table 20

7 Conclusion

We investigate how to effectively continue training LMs to improve upon their existing capabilities. Our experiments show that it is especially important to carefully define the data distribution and learning rate decay schedule used during continued pretraining so that the model is able to smoothly transition away from the pretraining distribution and better learn the newly emphasized data sources. With these findings we propose a general recipe that model developers can use in order to perform continued pretraining on top of their own LMs and show that for our base model, we are able to improve cumulative accuracy by over 18%. We hope that this will be a starting point to enable future LMs to be developed through the reuse of existing models rather than retraining from scratch.

Limitations

In the development of our continued pretraining recipe, we only experiment along the axes of data distributions and hyperparameter configurations. Although we did not include them within our study, there may be added benefit in exploring other aspects such as altering the learning algorithm. Additionally, given that our study is conducted on top of a model with a given configuration and which was pretrained using a certain data distribution, the results that we highlight are likely to not extrapolate well when used in settings highly divergent

525 from the one utilized in the study. Finally, we
526 limited our goal within continued pretraining to
527 improving the general purpose capabilities of the
528 pretrained model; however, there are many addi-
529 tional angles when considering model reuse such
530 as domain specialization and the efficient addition
531 of new knowledge into existing models.

532
533
534
535
536
537
538
539
540
541
542
543
544
545
546
547
548
549
550
551
552
553
554
555
556
557
558
559
560
561
562
563
564
565
566
567
568
569
570
571
572
573
574
575
576
577
578
579
580
581
582
583
584
585
586
587
588
589

References

Joshua Ainslie, James Lee-Thorp, Michiel de Jong, Yury Zemlyanskiy, Federico Lebrón, and Sumit Sanghai. 2023. GQA: Training Generalized Multi-Query Transformer Models from Multi-Head Checkpoints. *arXiv preprint arXiv:2305.13245*.

Zeyuan Allen-Zhu and Yuanzhi Li. 2023. [Physics of language models: Part 3.1, knowledge storage and extraction](#). *Preprint*, arXiv:2309.14316.

Anthropic. 2024. The Claude 3 Model Family: Opus, Sonnet, Haiku.

Cody Blakeney, Mansheej Paul, Brett W. Larsen, Sean Owen, and Jonathan Frankle. 2024. [Does your data spark joy? performance gains from domain upsampling at the end of training](#). *Preprint*, arXiv:2406.03476.

Tom B. Brown, Benjamin Mann, Nick Ryder, Melanie Subbiah, Jared Kaplan, Prafulla Dhariwal, Arvind Neelakantan, Pranav Shyam, Girish Sastry, Amanda Askell, Sandhini Agarwal, Ariel Herbert-Voss, Gretchen Krueger, Tom Henighan, Rewon Child, Aditya Ramesh, Daniel M. Ziegler, Jeffrey Wu, Clemens Winter, Christopher Hesse, Mark Chen, Eric Sigler, Mateusz Litwin, Scott Gray, Benjamin Chess, Jack Clark, Christopher Berner, Sam McCandlish, Alec Radford, Ilya Sutskever, and Dario Amodei. 2020. [Language models are few-shot learners](#). *Preprint*, arXiv:2005.14165.

Massimo Caccia, Pau Rodriguez, Oleksiy Ostapenko, Fabrice Normandin, Min Lin, Lucas Caccia, Issam Laradji, Irina Rish, Alexandre Lacoste, David Vazquez, and Laurent Charlin. 2021. [Online fast adaptation and knowledge accumulation: a new approach to continual learning](#). *Preprint*, arXiv:2003.05856.

Arslan Chaudhry, Marcus Rohrbach, Mohamed Elhoseiny, Thalaisyasingam Ajanthan, Puneet K. Dokia, Philip H. S. Torr, and Marc’Aurelio Ranzato. 2019. [On tiny episodic memories in continual learning](#). *Preprint*, arXiv:1902.10486.

Mark Chen, Jerry Tworek, Heewoo Jun, Qiming Yuan, Henrique Ponde de Oliveira Pinto, Jared Kaplan, Harri Edwards, Yuri Burda, Nicholas Joseph, Greg Brockman, Alex Ray, Raul Puri, Gretchen Krueger, Michael Petrov, Heidy Khlaaf, Girish Sastry, Pamela Mishkin, Brooke Chan, Scott Gray, Nick Ryder, Mikhail Pavlov, Alethea Power, Lukasz Kaiser, Mohammad Bavarian, Clemens Winter, Philippe Tillet, Felipe Petroski Such, Dave Cummings, Matthias Plappert, Fotios Chantzis, Elizabeth Barnes, Ariel Herbert-Voss, William Hebgen Guss, Alex Nichol, Alex Paino, Nikolas Tezak, Jie Tang, Igor Babuschkin, Suchir Balaji, Shantanu Jain, William Saunders, Christopher Hesse, Andrew N. Carr, Jan Leike, Josh Achiam, Vedant Misra, Evan Morikawa, Alec Radford, Matthew Knight, Miles Brundage, Mira Murati, Katie Mayer, Peter Welinder, Bob McGrew, Dario Amodei, Sam McCandlish, Ilya

Sutskever, and Wojciech Zaremba. 2021. [Evaluating large language models trained on code](#). *Preprint*, arXiv:2107.03374. 590
591
592

Aakanksha Chowdhery, Sharan Narang, Jacob Devlin, Maarten Bosma, Gaurav Mishra, Adam Roberts, Paul Barham, Hyung Won Chung, Charles Sutton, Sebastian Gehrmann, et al. 2022. PaLM: Scaling Language Modeling with Pathways. *arXiv preprint arXiv:2204.02311*. 593
594
595
596
597
598

DeepSeek-AI, :, Xiao Bi, Deli Chen, Guanting Chen, Shanhuang Chen, Damai Dai, Chengqi Deng, Honghui Ding, Kai Dong, Qiushi Du, Zhe Fu, Huazuo Gao, Kaige Gao, Wenjun Gao, Ruiqi Ge, Kang Guan, Daya Guo, Jianzhong Guo, Guangbo Hao, Zhewen Hao, Ying He, Wenjie Hu, Panpan Huang, Erhang Li, Guowei Li, Jiashi Li, Yao Li, Y. K. Li, Wenfeng Liang, Fangyun Lin, A. X. Liu, Bo Liu, Wen Liu, Xiaodong Liu, Xin Liu, Yiyuan Liu, Haoyu Lu, Shanghao Lu, Fuli Luo, Shirong Ma, Xiaotao Nie, Tian Pei, Yishi Piao, Junjie Qiu, Hui Qu, Tongzheng Ren, Zehui Ren, Chong Ruan, Zhangli Sha, Zhihong Shao, Junxiao Song, Xuecheng Su, Jingxiang Sun, Yaofeng Sun, Minghui Tang, Bingxuan Wang, Peiyi Wang, Shiyu Wang, Yaohui Wang, Yongji Wang, Tong Wu, Y. Wu, Xin Xie, Zhenda Xie, Ziwei Xie, Yiliang Xiong, Hanwei Xu, R. X. Xu, Yanhong Xu, Dejian Yang, Yuxiang You, Shuiping Yu, Xingkai Yu, B. Zhang, Haowei Zhang, Lecong Zhang, Liyue Zhang, Mingchuan Zhang, Minghua Zhang, Wentao Zhang, Yichao Zhang, Chenggang Zhao, Yao Zhao, Shangyan Zhou, Shunfeng Zhou, Qihao Zhu, and Yuheng Zou. 2024. [Deepseek llm: Scaling open-source language models with longtermism](#). *Preprint*, arXiv:2401.02954. 599
600
601
602
603
604
605
606
607
608
609
610
611
612
613
614
615
616
617
618
619
620
621
622
623

Ahmed El-Kishky, Vishrav Chaudhary, Francisco Guzmán, and Philipp Koehn. 2019. Ccaligned: A massive collection of cross-lingual web-document pairs. *arXiv preprint arXiv:1911.06154*. 624
625
626
627

Robert M. French. 1999. [Catastrophic forgetting in connectionist networks](#). *Trends in Cognitive Sciences*, 3(4):128–135. 628
629
630

Leo Gao, Stella Biderman, Sid Black, Laurence Golding, Travis Hoppe, Charles Foster, Jason Phang, Horace He, Anish Thite, Noa Nabeshima, Shawn Presser, and Connor Leahy. 2020. The Pile: An 800gb dataset of diverse text for language modeling. *arXiv preprint arXiv:2101.00027*. 631
632
633
634
635
636

Google DeepMind Gemma Team. 2024. Gemma: Open Models Based on Gemini Research and Technology. 637
638

Kshitij Gupta, Benjamin Thérien, Adam Ibrahim, Mats L. Richter, Quentin Anthony, Eugene Belilovsky, Irina Rish, and Timothée Lesort. 2023. [Continual pre-training of large language models: How to \(re\)warm your model?](#) *Preprint*, arXiv:2308.04014. 639
640
641
642
643
644

Suchin Gururangan, Ana Marasović, Swabha Swayamdipta, Kyle Lo, Iz Beltagy, Doug Downey,

B Experiments

The evaluation results across all considered tasks are shared below for each of our experiments.

Task	Pretrained Model
MMLU	59.3
HellaSwag	80.4
HumanEval	31.1
MGSM (ES, JA, TH)	24.9

Table 12: Model accuracy after 8T tokens of pretraining. We find that the model struggles on STEM based reasoning tasks due to its low scores on MGSM and STEM subtasks of MMLU.

B.1 Data Distribution

Table 13 shares the results across all tasks for each experiment mentioned within Section 5.1.

B.2 Learning Rate Schedule

In identifying a learning rate schedule for continued pretraining, we experiment with various degrees of warmup and values of $\eta_{max_{ct}}$. The combinations we consider are: warmup from η_{min} to $\eta_{max_{ct}} = 1.5 * \eta_{min}$, warmup from $0.5 * \eta_{min}$ to $\eta_{max_{ct}} = \eta_{min}$, and warmup from 0 to what the expected learning rate value would be had the pretraining learning rate schedule been extended to incorporate the continued training tokens (i.e., from 8T to 8.3T). We use η_{min} to specify the minimum learning rate value of the pretrained model, which is $4.5e-5$. Figure 6 highlights each of these schedules, and we note that these combinations were chosen to quantify different degrees of aggressiveness when using warmup in a continued pretraining learning rate schedule.

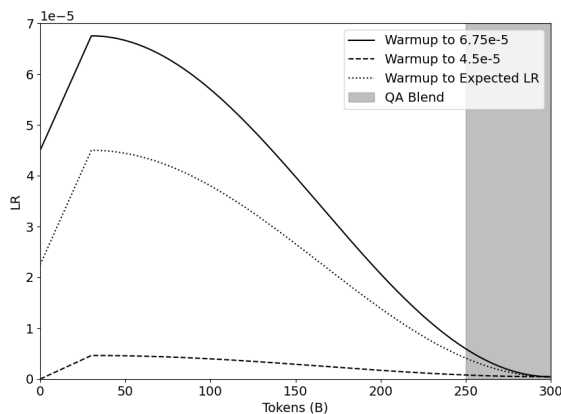


Figure 6: Cosine decay schedule with the various levels of warmup which we experiment with.

As highlighted in Table 15, we find that including any level of warmup within the continued training learning rate schedule causes regressions in evaluation accuracies, indicating that it is best to decay directly from η_{min} .

In addition to cosine annealing, we experiment with the WSD learning rate scheduler (Hu et al., 2024). Table 16 compares the best found setting of WSD with cosine annealing. The WSD schedule produces significantly lower evaluation accuracies than cosine annealing. We hypothesize that in continued pretraining, switching the decay schedule from the one used during pretraining is harmful. Hence, for models pretrained with cosine annealing, the learning rate schedule in continued training should also use cosine annealing.

B.3 Switch of Data Distributions

Table 18 highlights that the findings of our experiments in Section 5.3 also hold at the continued training token horizon of 100B tokens. This indicates that regardless of the number of continued training tokens, transitioning between the GB and QB distributions at $\frac{\eta_{max_{ct}}}{5}$ is optimal.

C Ablations

C.1 Varying Token Horizons

When extending the number of continued pretraining tokens to 1T, we found that our existing QB distribution would cause the small QA dataset to be trained on for a large number of epochs. To correct for this, we reduce the weight on the QA dataset so that it would be trained on for no more than 4 epochs. Figure 7 demonstrates the distribution of the QB when used at the scale of 1T continued pretraining tokens.

Data Blend	MMLU	HellaSwag	HumanEval	MGSM (ES, JA, TH)
Pretraining	61.9	81.2	28.1	34.7
QA	62	78.7	32.9	40.1
Pretraining (250B) + QA (50B)	62.6	82.2	29.9	42.4
Pretraining	61.9	81.2	28.1	34.7
Reweight Domains	61.9	81.7	29.9	33.2
Pretraining w/ High Quality Web	62.2	80.9	34.1	32.9
No Web	62.3	81.8	29.9	37.7
Upweight Non Web w/ High Quality Web	62.6	81.4	31.7	32.1
QA 1	63.0	82.4	29.9	41.9
QA 2 (+STEM, +World Knowledge)	63.9	82.3	29.3	36.7
QA 3 (+STEM, +Chat)	64.1	82.2	28.7	44.7
QA	64.2	82.4	30.5	44.5
QA w/ Upweighted STEM	64.1	82.3	28.1	42.9
QA w/ 1.5e QA data	64.1	82.2	28.7	44.7
QA w/ 3.5e QA data	64.4	27.4	82.4	43.3

Table 13: Per-task evaluation results of each experiment mentioned within Section 5.1 on defining data distributions for continued pretraining.

LR Schedule	MMLU	HellaSwag	HumanEval	MGSM (ES, JA, TH)
Decay to $\frac{\eta_{max_{ct}}}{10}$	63.9	82.4	29.3	43.7
Decay to $\frac{\eta_{max_{ct}}}{100}$	64.2	82.2	31.1	45.2
Decay to 0	64.2	30.5	82.4	44.5

Table 14: Per-task evaluation results of the experiments mentioned in Table 8 on identifying an appropriate learning rate decay schedule for continued pretraining.

LR Schedule	MMLU	HellaSwag	HumanEval	MGSM (ES, JA, TH)	Avg. Acc.
Warmup to $6.75e-5$	64.0	81.9	31.1	42.3	54.8
Warmup to $4.5e-5$	64.0	82.1	32.9	41.5	55.1
Warmup to Expected LR	63.3	82.1	31.7	42.5	54.9
No Warmup	64.2	31.1	82.2	45.2	55.7

Table 15: Comparison of including warmup within learning rate schedules for continued pretraining. No warmup achieves the best evaluation results.

LR Schedule	MMLU	HellaSwag	HumanEval	MGSM (ES, JA, TH)	Avg. Acc.
WSD	63.6	80.2	28.1	39.5	52.8
Cosine Annealing	64.2	82.2	31.1	45.2	55.7

Table 16: We find that WSD causes significant regression in evaluation accuracy compared to cosine annealing. Both learning rate schedules were decayed till $\frac{\eta_{max_{ct}}}{100}$.

Distribution Switch	MMLU	HellaSwag	HumanEval	MGSM (ES, JA, TH)
At $\eta_{max_{ct}}$ (from step 0)	65.0	78.7	29.9	37.7
At $\frac{\eta_{max_{ct}}}{2}$	60.9	81.6	32.3	44.1
At $\frac{\eta_{max_{ct}}}{5}$	63.8	82.2	32.3	46.1
At $\frac{\eta_{max_{ct}}}{10}$	63.9	82.2	29.3	44.7
At $\frac{\eta_{max_{ct}}}{50}$	63.3	81.6	31.1	42.3

Table 17: Per-task evaluation results of the experiments mentioned in Table 9 on how to switch between data distributions in continued pretraining.

Distribution Switch	MMLU	HellaSwag	HumanEval	MGSM (ES, JA, TH)	AVG
At $\eta_{max_{ct}}$ (from step 0)	64.1	79.2	31.1	40.0	53.6
At $\frac{\eta_{max_{ct}}}{2}$	63.2	81.6	27.4	44.1	54.1
At $\frac{\eta_{max_{ct}}}{5}$	63.0	81.9	31.7	43.6	55.0
At $\frac{\eta_{max_{ct}}}{10}$	63.6	81.8	30.5	39.7	53.9
At $\frac{\eta_{max_{ct}}}{50}$	63.3	81.6	31.1	42.3	54.6

Table 18: Ablation of the data distribution switch experiments at a continued pretraining scale of 100B tokens. As found for the 300B token continued training horizon, switching distributions at $\frac{\eta_{max_{ct}}}{5}$ achieves the highest accuracy.

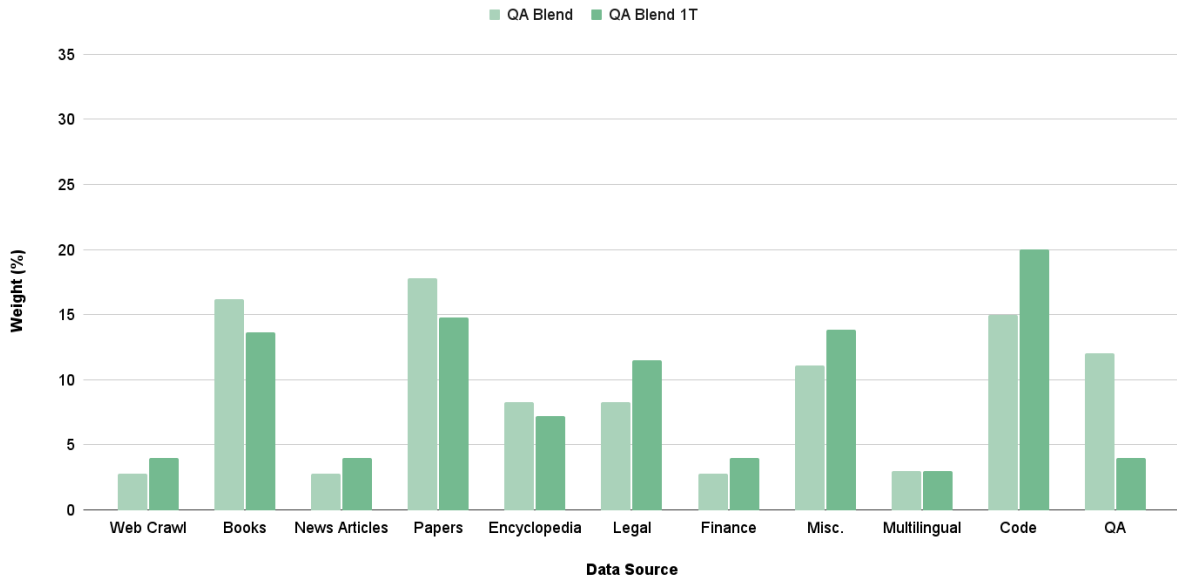


Figure 7: Distribution of the QB blend when extending the number of continued pretraining tokens to 1T.

Num CT Tokens	MMLU	HellaSwag	HumanEval	MGSM (ES, JA, TH)	AVG
0B	59.3	80.4	31.1	24.9	48.9
100B	63.0	81.9	31.7	43.6	55.0
300B	63.8	82.2	32.3	46.1	56.1
1T	65.3	82.4	34.1	45.5	

Table 19: Per-task evaluation results of the experiments mentioned in Table 11 on how the identified continued pretraining recipe performs at varying amounts of continued training tokens.

Blend	MMLU	HellaSwag	HumanEval	MGSM (ES, JA, TH)
CT 1T	65.3	82.4	34.1	45.5
CT 1T w/ Mined Docs	66.6	81.7	36.6	46.7

Table 20: Per-task evaluation results of the experiments mentioned in Table 11 on how document mining increases the utility of existing data sources in continued pretraining.